LAWRENCE
LIVERMORE
NATIONAL
LABORATORY

LLNL-CONF-418041

Assessment and Mitigation of Electromagnetic Pulse (EMP) Impacts at Short-pulse Laser Facilities

C. G. Brown, Jr., E. Bond, T. Clancy, S. Dangi, D. C. Eder, W. Ferguson, J. Kimbrough, A. Throop

October 14, 2009

Inertial Fusion Sciences and Applications (IFSA)
San Francisco, CA, United States
September 6, 2009 through September 11, 2009

Disclaimer

Assessment and Mitigation of Electromagnetic Pulse (EMP) Impacts at Short-pulse Laser Facilities

C G Brown Jr., E Bond, T Clancy, S Dangi, D C Eder, W Ferguson, J Kimbrough, A Throop

Lawrence Livermore National Laboratory, 7000 East Ave., Livermore, CA 94550, USA

E-mail: brown207@llnl.gov

Abstract. The National Ignition Facility (NIF) will be impacted by electromagnetic pulse (EMP) during normal long-pulse operation, but the largest impacts are expected during short-pulse operation utilizing the Advanced Radiographic Capability (ARC). Without mitigation these impacts could range from data corruption to hardware damage. We describe our EMP measurement systems on Titan and NIF and present some preliminary results and thoughts on mitigation.

1. Introduction

Electromagnetic pulse (EMP) is a known issue for short-pulse laser facilities such as Vulcan, Titan and Omega-EP [1]. We expect the National Ignition Facility (NIF) will be impacted by EMP in both long-pulse, which is the normal NIF operation mode, and short-pulse operation. However, we expect the largest impacts during short-pulse operation, such as with the short-pulse based Advanced Radiographic Capability (ARC). Therefore, understanding and mitigating EMP is an important part of the effective use of these and other laser facilities. Short-pulse ($\sim$ few ps) lasers produce very energetic (MeV) electrons that can be used to produce short-pulse, high-energy, x-ray backlighting as in ARC experiments. In general, the high energy of these electrons causes more to escape the target than the lower-energy "hot electrons" ($<$100 keV) produced by laser-plasma interactions in long-pulse ($\sim$ few ns) laser-plasma interactions.

Even in the case of short-pulse operation, the number of electrons that escape ($\sim 10^{12}$) is a small fraction of the total number produced in the target, and the associated charge is a small fraction of a Coulomb. However, the short duration causes the escaping electrons to produce very large transient currents and EMP. In addition, the short duration translates to a very broad spectrum with the potential of high-frequency EMP. In both cases (short and long pulse) escaping electrons can be a significant source of EMP.

For effective shielding it is critical that the spectrum of the EMP, as well as the time-domain behavior, is known. Both measurements and simulations are necessary to understanding EMP in short- and long-pulse lasers. We have fielded a large suite of diagnostics, including B- and D-dot sensors, inside and outside the Titan short-pulse laser target chamber, which is a part of the Jupiter Laser Facility at Lawrence Livermore National Laboratory (LLNL) [2], in order to characterize both the EMP and the escaping electrons. We have used our Titan experience to

field an EMP measurement system with B- and D-dot sensors inside and outside of NIF's target chamber. In order to establish predictive capabilities and improve mitigation techniques, we have extended the 3D electromagnetic simulation code EMSolve [3] to model EMP generation. A specified number and spatial distribution of escaping electrons are used as input to EMSolve simulations. In this paper we describe our measurement systems on Titan and NIF; the signal processing techniques we employ; and give some preliminary results and thoughts on mitigation. Refer to [4] for information how we model EMP in EMSolve.

2. Measurement systems

We fielded a wide variety of diagnostics in Titan in order to understand EMP inside short-pulse lasers. Our diagnostics include multiple B- and D-dot sensors, electron spectrometers, TLD's (Thermo-Luminescent Detectors), UTLD's (Ultra-Thin TLD's), image plates, and a Faraday cup. Our B- and D-dot measurement system is well shielded, consisting of differential sensors for common-mode noise rejection; shielded conduit to attenuate fields impinging on baluns and measurement cables; and a shielded box for the oscilloscopes. We have B-dot sensors both inside and outside the laser chamber and a D-dot sensor inside to measure the levels of electromagnetic fields. It is important to measure both the time-varying magnetic and electric fields because the ratio of those fields inside resonant chambers generally is not the intrinsic impedance of free space (377Ω). Figure 1 is a photograph of the interior of the Titan chamber. A Prodyn RB-270 B-dot sensor (mid frequency); two RB-230 B-dot sensors (high frequency); and a Prodyn AD-55 D-dot are located in the top, center, and right areas of the photograph. The remaining interior sensor in the picture, a Prodyn RB-50 sensor (low frequency), is located in the top, left portion of the photograph.

Our NIF EMP measurement system is similar. The present configuration in NIF is a temporary early deployment for initial NIF operation that does not provide the full Faraday-cage shielding that was used on Titan. However, measurements with sensors covered with electromagnetic shielding indicate little, if any, corruption due to extraneous EMP noise in the present configuration. A well-shielded measurement system, similar to the Titan system, is being installed for longer-term operation.

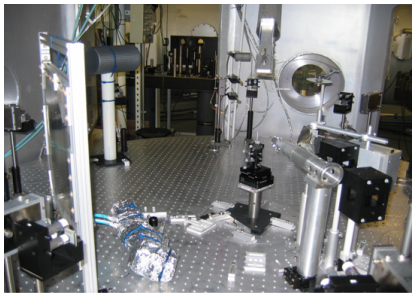

Figure 1. Inside of Titan chamber during our measurement campaign.

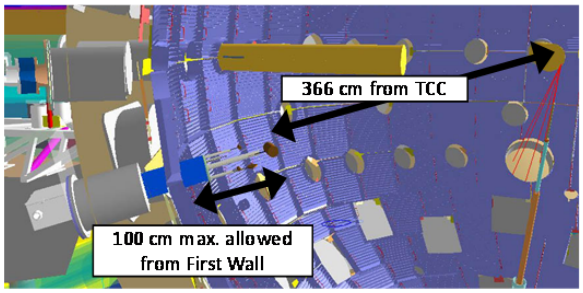

Figure 2. CAD image of EMP diagnostic in target chamber.

3. Signal processing techniques

In order to remove the effects of the measurement system we perform channel compensation, or deconvolution. We construct calibration files for each component of the measurement system, consisting of sampled transfer functions in the frequency domain. The measurement system transfer function is then simply the product of all of the frequency-domain transfer functions of the individual components. A straight-forward method of performing the channel compensation would be to transform the data from the oscilloscopes into the frequency domain; apply the inverse of the system transfer function; and then transform back into the time domain. However,

this method tends to magnify noise in the frequency bands where the transfer function is small, producing unrealistic signals. In order to reduce this noise magnification, we use Tikhonov regularization with L-curve analysis to determine the optimal regularization parameter [5]. Additionally, we low-pass filter the channel-compensated signal at the frequency of the analog low-pass filter in the measurement system.

4. Preliminary results and thoughts on mitigation

We applied the signal processing techniques above to the measured data from Titan and NIF. First, our preliminary results from short-pulse Titan ($\sim$ ps) indicate large EMP, on the order of tens to hundreds of kV/m, that has a duration (before decaying into the noise) of up to about a few hundred ns. For example see Fig. 3, which is processed data from one of our RB-230 (high-frequency) sensors located about 32 cm from target chamber center (TCC). The resulting magnetic flux density values (B field) have been converted to electric field strength (E field) by multiplying by c, the speed of light in vacuum: $E \approx cB$. Note that this conversion is only approximate, since the relationship does not hold in general for resonant cavities. The peak magnitude of the resulting E-field signal is 167 kV/m. The transient duration before decaying into the noise is $\sim$ 400 ns. An estimate of the one-sided power spectral density (PSD), using Welch's method on just the transient portion is displayed in Fig. 4. The PSD indicates significant EMP out to greater than $\sim$ 5 GHz. We cannot observe the upper frequency of the range because of the oscilloscope analog bandwidth and an anti-aliasing low-pass filter in the measurement system. Further, we have observed a clear trend with target size in the Titan data (Fig. 5). Note that the peak magnitude of the E field tends to increase with the target size, a possible explanation being that a larger target reduces the electrostatic field allowing more electrons to escape. The data in Fig. 5 is for square silver targets 12 μm thick. The laser pulse width is 2 ps with laser energies ranging from 123 to 155 J ($\sim$ 75 TW average power).

Our preliminary results from long-pulse ($\sim$ ns) NIF indicate EMP with peak magnitudes up to $\sim$ 10 kV/m. For example see Figs. 6, 7, and 8 which are processed data from our RB-230 (high-frequency), RB-270 (mid-frequency), and RB-50 (low-frequency) sensors, respectively, located about 4 m from TCC. The shot is `N090808` (233 kJ, 2 ns, 116 TW, vacuum hohlraum). Note that if we assume $1/r^2$ scaling, the fields could be $\sim 16\times$ higher 1 m from TCC. As for the Titan data, the measured B-field values have been converted to E field using $E \approx cB$. An estimate of the one-sided PSD, using Welch's method on just the transient portion of the signals is displayed in Fig. 9. The PSD is plotted for the different sensors only over the frequency range where they are "valid", which is judged by comparison with the noise floor. The PSD indicates EMP out to greater than $\sim$ 5 GHz. As before we cannot observe the upper frequency of the range because of the oscilloscope analog bandwidth and an anti-aliasing low-pass filter in the measurement system. Also, we measured volt-level noise, likely due to EMP, on terminated signal cables on a NIF diagnostic instrument manipulator (DIM) inside the target chamber. We have not yet measured any EMP above the noise outside of the target chamber.

Based on these preliminary findings, shielding for diagnostics inside the target chamber is being reassessed, starting the process of preparation for ARC operation, which we estimate could produce approximately an order of magnitude higher fields. Given the high-frequency content of the measured EMP, the present focus of mitigation efforts is on placing Faraday-cage shielding around cables and diagnostics inside the target chamber. Currently, we estimate that 60 dB of shielding is required for the DIM signal cabling, and flexible shielded conduits and other shielding methods are being evaluated for this purpose. Similarly, we are providing Faraday-cage shielding for airboxes and diagnostics mounted on the DIMs. Carefully designed fingerstock contacts on the DIMs are being installed to control EMP-induced currents and to mitigate potential arcing and wear. The use of ferrites to address low-frequency EMP currents is also being explored; these may be more useful if EMP fields outside of the target chamber

become a problem, e.g. possibly during ARC operation. Mesh and electromagnetic interference (EMI) windows are being evaluated for use where cameras must be enclosed in shielding.

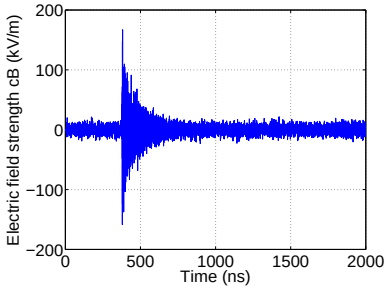

Figure 3. Processed Titan data from high-frequency B-dot sensor (with $E \approx cB$).

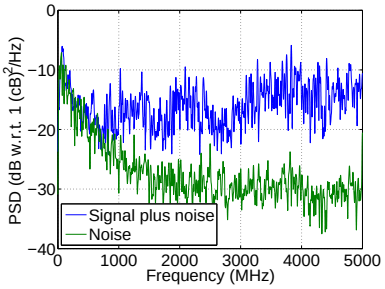

Figure 4. An estimate of the PSD of the transient portion of Fig. 3.

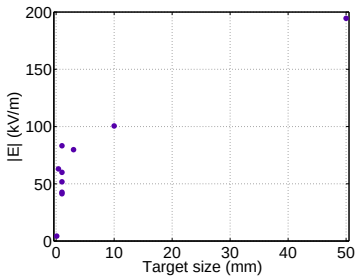

Figure 5. Peak magnitude of electric field in Titan versus target size.

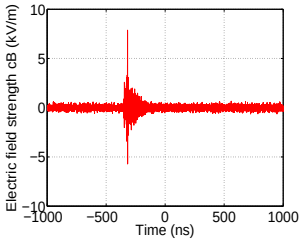

Figure 6. Processed NIF data from high-frequency B-dot sensor (with $E \approx cB$).

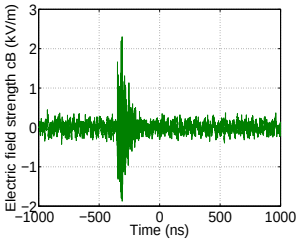

Figure 7. Processed NIF data from mid-frequency B-dot sensor (with $E \approx cB$).

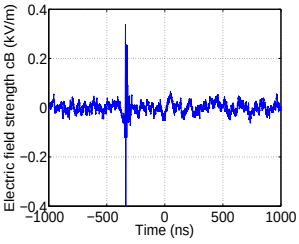

Figure 8. Processed NIF data from low-frequency B-dot sensor (with $E \approx cB$).

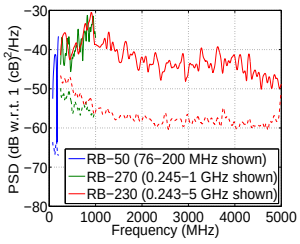

Figure 9. Composite spectrum of processed NIF data and noise floor from Figs. 6 to 8.

5. Summary and conclusions

We have deployed measurement systems on both Titan and NIF. Our preliminary data from Titan indicate high-level (on the order of tens to hundreds of kV/m), broad-spectrum EMP. We have also observed a clear trend in EMP level with target size. Our preliminary data from long-pulse NIF indicates EMP up to ~ 10 kV/m, which we estimate to be higher (~ 100 kV/m) near TCC. We postulate that these fields are generating the volt-level signals that we are observing on the diagnostic cables. Based on these preliminary findings, shielding for target chamber diagnostics is being reassessed, starting the process of preparation for ARC operation.

Acknowledgments

Prepared by LLNL under Contract DE-AC52-07NA27344. The authors are grateful for the assistance of the Jupiter Laser Facility staff, including Jim Bonlie, Roger Van Maren, Dwight Price, and others. Many other individuals from both National Security Technologies, LLC (NSTec), Zaheer Ali, Craig Brooksby, Jeff Fornes, Larry MacNeil, Ken Moy, Vu Tran, and John Yuhas, and LLNL, Bill DeHope, also contributed to this effort. We are grateful for their help, too. Finally, we are indebted to the entire NIF team.

References

[1] Mead M J, Neely D, Gauoin J, Heathcote R and Patel P 2004 *Rev. Sci. Instrum.* **75** 4225
[2] http://jlf.llnl.gov (Accessed September 2009)
[3] White D and Stowell M 2004 *IEEE T. Microw. Theory* **52**(5) 1404
[4] Stowell M L, Brown C G, Eder D C and White D A 2009 in this conference series
[5] Aster R, Borchers B and Thurber C 2005 *Parameter Estimation and Inverse Problems* (Academic Press)